SPE Improved Oil Recovery Conference, Tulsa, Oklahoma, USA, 21 – 23 April 2026.

SPE 231553-MS

# Examining the Desaturation Potential of Low and High-Salinity Viscoelastic Polymer Solutions at High Salinity and High Temperature Carbonate Reservoir Conditions

**Dirie Dhahir[1], Madhar Sahib Azad[1, 2], Subhash Ayirala[3], Randall S. Seright[4], Dhafer Al Shehri[1,2], Mohammad Alotaibi[3]**

[1]Department of Petroleum Engineering, College of Petroleum Engineering and Geosciences (CPG), King Fahd University of Petroleum & Minerals, KFUPM, Dhahran 31261, Saudi Arabia

[2]Center for Integrative Petroleum Research (CIPR), College of Petroleum Engineering and Geosciences (CPG), King Fahd University of Petroleum & Minerals, KFUPM, Dhahran 31261, Saudi Arabia

[3]Exploration and Petroleum Engineering Centre - Advanced Research Centre (EXPEC-ARC), Saudi Aramco

[4]New Mexico Institute of Mining & Technology

## Abstract

Over the last two decades, high interest has been shown to explore whether viscoelastic polymer solutions can reduce the capillary-trapped residual oil saturation (Sor) under practical reservoir conditions. To characterize this relatively less explored potential and identify the mechanisms that contribute to Sor reduction, we measured capillary desaturation curves (CDC) for viscoelastic polymer solutions, along with the evaluation of their ability to alter wettability. The studies were performed using both low- and high-salinity viscoelastic polymer solutions at high salinity and high temperature carbonate reservoir conditions.

A combination of bulk and in-situ rheological measurements, contact angle experiments, and desaturation experiments were conducted. Desaturation experiments were performed using 2500-ppm and 4000-ppm acrylamide-ATBS-copolymer solutions prepared in 5760-ppm-TDS and 57600-ppm-TDS brines in 105-to-111-mD oil-wet limestone cores saturated with 2.8-cP oil and 257600-ppm formation brine at 95°C. The desaturation experiments involved: a) performing bump water flooding up to 64 ft/day and a subsequent sequential glycerin flood to ensure that the residual oil was highly discontinuous and strongly trapped, and the core was well-swept; and b) initiating the desaturation process with polymer solutions using an imposed flux of 0.05 ft/day and continuing up to 100 ft/day.

Bump water flooding with high salinity brine and glycerin flood reduced the oil saturation by 25-30% in both experiments. At low flux rates (from 0.05 ft/day to 1 ft/day), both low and high salinity polymers did not reduce the oil saturation further. Such behavior is observed even though a) the shear thickening onset was noted at 0.25 ft/day for both solutions, and b) a slight reduction in contact angle (2-to-7 degrees) was observed. At 5 ft/day, both low and high polymer solutions showed a noticeable reduction in Sor—at computed critical capillary numbers of $4.0 \times 10^{-5}$ and $4.82 \times 10^{-5}$, respectively. Increasing the flux rate further up to 100 ft/day resulted in significant further oil desaturation, yielding additional residual oil recoveries of ~13% for the low salinity polymer solution and ~11% for the high salinity polymer solution. Although Sor reduction was observed at 5 ft/day in the lab, calculations indicate that achieving a flux above 5 ft/day in the target reservoir application and a significant Sor reduction would only be accomplished within ~30 ft from the wellbore.

In this work, CDC curves for low and high-salinity viscoelastic polymer solutions were reported for the first time under high salinity and high temperature oil-wet carbonate conditions. Examinations and interpretations of the developed CDC curves indicate that the observed Sor reduction in the lab cannot be expected in the carbonate reservoirs for the well spacings typically used for polymer flood projects.

## Introduction

Polymer flooding is one of the most widely applied chemical enhanced oil recovery (cEOR) methods, commonly used in tertiary mode to increase oil recovery in depleted water-flooded reservoirs. Some successful polymer flood projects in recent years include Milne Point in Alaska (Zhao et al. 2021), Pelican Lake in Canada (Delamaide et al. 2014), Dalia in Angola (Morel et al. 2008), Tambaredjo in

Suriname (Moe Soe Let et al. 2012), Captain in the UK (Poulsen et al. 2018), Kalamkas project in Kazakhstan (Sagyndikov et al. 2018). More details on polymer flood field projects in different reservoirs can be found in the works of Sagyndikov et al. (2022). Primarily, a polymer flood is used to accelerate recovery by improving sweep efficiency and reducing the mobility ratio between oil and water (Green and Willhite 2018; Seright and Wang 2023). The effectiveness of polymer flooding over water flooding is classically attributed to enhanced oil flow, delayed water breakthrough, lower water cut, and faster production of mobile oil (Sorbie 1991). Note that mobile oil refers to oil that is not well-swept, whereas residual oil is swept but trapped by capillary forces high enough to impede mobilization through a series of pores and pore bodies.

The oil recovery factor is the product of volumetric sweep efficiency and microscopic displacement efficiency. Sweep efficiency quantifies the amount of oil that is well-swept relative to the total volume of oil. It increases as more injected fluid contacts the oil within the reservoir and is hence a function of time (Green and Willhite 2018). By contrast, microscopic displacement efficiency is a pore-scale phenomenon that describes the amount of well-swept oil that is mobilized relative to the total amount of well-swept oil, where well-swept oil refers to oil contacted by the previous flooding. A conventional belief is that polymer flooding cannot recover the well-swept capillary-trapped oil beyond that recovered by the preceding water flood. This is based on the classical capillary number concept, which relates macroscopic viscous forces to capillary forces. EOR polymers do not substantially affect oil-water interfacial tension (IFT) (Clarke et al. 2016; Azad and Trivedi 2021) and therefore cannot reduce capillary forces through IFT reduction. By contrast, the use of highly concentrated, high-molecular-weight polymers in the Daqing oilfield reported an incremental recovery factor of 20% of the original oil in place (OOIP), which is twice the amount reported during conventional polymer flooding and comparable to recovery expectations for alkaline-surfactant polymer flooding (Wang et al. 2011). Since then, various laboratory polymer flood experiments have been conducted worldwide to investigate the effect of viscoelastic polymer flooding on residual oil saturation (Sor) reduction. These studies include those conducted by Urbissinova et al. 2010; Seright et al. 2011; Ehrenfried 2013; Vermolen et al. 2014; Clarke et al. 2016; Koh et al. 2018; Qi et al. 2017; Seright et al. 2018; Azad and Trivedi 2020a; 2020b; 2021; Barri et al. 2023. Careful examination of those studies indicates two main facts: (a) most studies reporting a positive influence of polymer viscoelastic effects are conducted at high-pressure/high-flux conditions, and (b) some studies fail to report Sor reduction even at the lab scale (Vermolen et al. 2014; Sandengen et al. 2017). For more details about the operational and petrophysical conditions associated with viscoelastic polymer flood lab studies, please refer to Table S-2 of Azad and Seright (2025). Azad and Seright (2025) compiled major polymer flood projects across the globe and reported that (a) the average velocity of the propagating polymer solutions in those typical projects is in the range of 0.02 to 0.05 ft/day, and (b) the average pressure gradient is in the range of ~3 to 10 psi/ft. Further, the authors reported that the average velocity of injected polymer solutions in the field is lower than the velocity needed for similar polymer solutions to exhibit shear-thickening viscoelastic effects (Figure 15 of Azad and Seright (2025)).

Shear thickening is one of the four flow regimes exhibited by EOR polymer solutions in porous media. Shear thickening is the phenomenon in which injected viscoelastic polymer solutions exhibit an increase in apparent viscosity in porous media with respect to an increase in the flux rate after a critical flux/shear rate called viscoelastic onset rate. Shear thickening is preceded by the Newtonian and shear-thinning regimes and followed by the mechanical degradation regime. While Newtonian and shear-thinning regimes are associated with both viscous polymeric flow (such as those associated with xanthan gum) and viscoelastic polymeric flow (such as those associated with HPAM), significant shear thickening and the subsequent mechanical degradation regime are associated only with viscoelastic polymeric flow in porous media (Seright et al. 2011; Clarke et al. 2016; Azad and Trivedi 2020a; 2021; Seright et al. 2023; 2025).

Besides shear-thickening viscoelastic effects, localized extensional effects and wettability alteration were perceived to influence oil recovery during viscoelastic polymer flooding (Azad and Trivedi 2019a; 2020b; 2021). At the pore scale, 75% of deformation is attributed to polymer elongation (Durst et al. 1987). Extensional viscosity was reported by Azad and Trivedi (2020b) to be higher for high-Mw, low-concentration polymer, resulting in higher Sor reduction when compared to low-Mw, high-concentration polymer (Clarke et al. 2016). This is despite the relatively lower shear and apparent viscosity possessed by high Mw-low concentrated polymer solutions when compared to the low Mw-high concentrated polymer solutions at the flooding rate of interest (Clarke et al. 2016). Azad and Trivedi (2021) developed a new capillary incorporating localized extensional rheological parameters that has a better correlation with Sor reduction than the one computed with the macroscopic viscosity (Figure 12 in Azad and Trivedi (2021)). Further, Azad and Seright (2025) examined the Chinese polymer projects compiled by Guo et al. (2021) in detail and reported that the Daqing polymer flood resulted in a higher recovery factor despite possessing a similar average velocity when compared to other projects (Figure 8 in Azad and Seright (2025)). The authors also cited the works of Souayeh et al. (2021) and Amiri et al. (2022) and discussed the importance of wettability alteration associated with the injection of polymer solutions in both oil-wet and water-wet rocks. These short compilations indicate that the polymer's viscoelastic effect on Sor reduction is a complex process with controversial aspects and entails the need to consider other phenomena, such as the wettability-altering potential of polymer solutions.

The controversy in polymer's viscoelasticity effect on Sor arises mainly because microscopic recovery is not a straightforward and easy process; it is influenced by multiple variables such as wettability, IFT, pore aspect ratio, permeability, displacing fluid flux, and oil

viscosity. Further, the porous media viscoelasticity is also a complex phenomenon that is influenced by extensional flow and non-linear viscoelasticity effects (Azad and Trivedi 2019a,b; 2020b; 2021; Azad 2023; 2024). Due to these complexities and the inherent contradiction, Seright (2017) suggested a case-by-case evaluation on the influence of viscoelastic polymer flooding on Sor.

Most polymer flooding projects were implemented in sandstones (Shuler et al. 1987; Wang et al. 2000; Morel et al. 2008; Al-Saadi et al. 2012; Delamaide et al. 2014; Zechner et al. 2015; Poulsen et al. 2018; Sagyndikov et al. 2018; Shankar et al. 2018). In recent past, interest has shifted towards exploring the potential of polymer flooding in carbonates (Al-Amrie et al. 2015; Jouenne 2020). This was made possible by the synthesis of thermally stable and high-salinity tolerant polymers such as sulfonated HPAM polymers (Vermolen et al. 2011; Seright et al. 2021). Although several lab investigations were conducted to determine the viscoelastic influence on Sor reduction in sandstones, only limited studies including those from our own work, were performed in carbonate cores (Lee et al. 2019; Dafaalla et al. 2025). The inherent difference between sandstones and carbonates not only stems from the differences in physico-chemical variables such as temperature, salinity, and heterogeneity, but also the rock wettability, which itself is a complex variable. Wettability influences the microscopic recovery and fluid distributions. Since carbonate reservoirs tend to be extremely oil-wet to mixed-wet, it is important that specific experimental studies with porous media of representative wetting nature are required.

In our previous study, we employed polymer flux rates of 4, 20, and 32.5 ft/day (Dafaalla et al. 2025) to study the polymer's viscous and viscoelastic influence on accessible oil recovery from heterogeneous unconsolidated carbonates. A careful examination of the polymer floods across the globe by Azad and Seright (2025) indicate that field relevant flux rates that represent the typical well spacings are 0.02-0.05 ft/day. It is important to study the influence of polymer viscoelasticity on Sor at these low fluxes for two reasons. Firstly, the low fluxes are field representative and have practical relevance for the typical well-spacings. Secondly, the scientific aspects of viscoelasticity are that they become dominant at higher fluxes at least up to the flux corresponding to the onset of the mechanical degradation regime due to lower observation time that the fluids are forced to reside in the pores (Azad and Trivedi 2019b; Jouenne and Heurteux 2020; Seright et al. 2025). Some studies convey that wettability alteration can play a role during polymer flooding in carbonates (AlSofi et al. 2018; Li et al. 2020; Souayeh et al. 2021). Wettability alteration by polymers becomes dominant at low salinity when compared to high salinity (Souayeh et al. 2021) and a case-by-case investigation of viscoelastic polymer solutions on Sor reduction along with the examination of wettability alteration potential with the injected salinity thereby becomes important.

Capillary desaturation curves (CDC) are a function of dimensionless capillary number (Nc) and Sor (Green and Willhite 2018). Nc correlates the displacing fluid's potential with Sor reduction during various EOR methods. Several authors in the past have explored the correlation between Nc and Sor from core flooding lab experiments (Dombrowski and Brownell 1954; Moore and Slobod 1956; Taber 1969; Abrams 1975; Chatzis and Morrow 1984; Chatzis et al. 1988). Different versions of capillary number were developed since the introduction of vis-cap concept by Moore and Slobod (1956) to account for the relevant variables involved in Sor reduction. For instance Azad and Trivedi (2021) developed a new capillary number incorporating extensional rheological parameters to account for the viscoelastic polymer's Sor reduction potential. The classical works of Taber (1980; 1981) discuss different variants of Nc.

The capillary number definition adopted in this work is from Stegemeier (1976).

$$N_C = \frac{k\Delta P}{L\sigma} \quad \text{..... Eq (1)}$$

Where $k$ is the core absolute permeability in mD, $\Delta P/L$ is the differential pressure gradient in psi/ft, and $\sigma$ is the IFT between oil and the displacing fluid in mN/m. The units described are the measured units from the conducted experiments. The dimensionless capillary number was calculated using conversion factors which were mD to m² for permeability, psi/ft to N/m²/m for differential pressure gradient, and mN/m to N/m for IFT. In this work, to cover the representative field flux rates (Azad and Seright 2025), as well as to examine the impact of wettability alteration on Sor reduction in typical harsh carbonates (high salinity, high temperature and extremely oil-wet), the development of capillary desaturation curves (CDC) is attempted using both low and high-salinity viscoelastic polymer solutions in the aged limestone cores. The aging process was done at 75°C, to ensure that the rocks become strongly oil-wet (Al-Ameer et al. 2023). The development of CDC curves for oil-wet carbonate rocks during viscoelastic polymer flooding is the prime objective of this study. The CDC curves were generated for water flooding, low concentration-low salinity polymer, and high concentration-high salinity polymer. We conducted constant-rate core flooding experiments to develop the CDC for both low- and high-salinity viscoelastic polymer solutions with varying concentrations. The concentrations are varied to ensure that the injected polymer solutions have similar Newtonian viscosity, since it was also aimed to compare the viscoelastic potential of low and high salinity polymer solutions to recover residual oil at the field-relevant fluxes. The polymer flooding fluxes used for generating CDC range from 0.05 to 100 ft/day, at a temperature of 95°C, formation water salinity (TDS) of 213,734 ppm, and preceding bump water flooding was performed up to 64 ft/day. The preceding water flooding was done with bump mode to ensure that the oil becomes highly discontinuous and trapped. The preceding bump water flooding was followed by the glycerin flood to ensure that any mobile oil after the bump water flooding gets recovered so that we could examine true Sor reduction of viscoelastic polymer solutions at low and high salinity injection conditions. Therefore, it is important to note that the CDC development and the subsequent viscoelastic polymer potential on Sor reduction is studied

at harsh carbonate conditions- including high temperature/ high formation water salinity, extreme low fluxes, high oil-wetting nature, and on highly discontinuous trapped oil. The contact angle measurements are also performed to quantify the impact of injected polymer solutions on wettability altering potential at harsh conditions. The in-situ rheological experiments are performed with low and high salinity viscoelastic polymer solutions to track the flow regimes and to aid the interpretation. The results are interpreted both scientifically and pragmatically to examine whether the harsh carbonate reservoirs can reap the benefits of Sor reduction at the field-scale due to low and/or high salinity polymer's viscoelasticity and wettability altering potential.

## Methodology

### Porous media

Various Indiana limestone cores were used in this work; all the cores had a 1.5-inch diameter. For core flooding experiments, 4 cores were used. Oil desaturation core floods used ~ 4-inch-long cores NIL-06 and NIL-09 with brine permeability of 110.9 and 104.8 md, respectively. For the in situ rheological characterization, composite cores were used ~ 10-inch-long cores NIL-15 and NIL-16, with brine permeability of 100.4 and 118.9 md, respectively. According to Darcy's law, for the same fluid viscosity, injection rate, core cross-sectional area, and permeability, pressure drop is directly proportional to the core length. We selected 10-inch cores to increase the pressure drop readings at the same injection rate. This was followed specifically to obtain lower pressure drops at low Darcy flux rates of 0.05-0.1 ft/day. The pressure-drop readings depend on the differential transducer pressure accuracy and will be explained later. Porosity measurements were conducted using a helium porosimeter, and brine permeability was measured in the core flood system as described in Fig. 1. The measured properties of Indiana limestone cores are shown in Table 1.

| Sample ID | Porosity (%) | Brine Permeability (mD) | Pore volume (ml) | Length (cm) | Experiment |
|---|---|---|---|---|---|
| NIL-06 | 23.7 | 110.9 | 24.7 | 10.4 | Low concentration-low salinity polymer oil desaturation |
| NIL-09 | 22.7 | 104.8 | 23.5 | 10.4 | High concentration-high salinity polymer oil desaturation |
| NIL-15 | 21.9 | 100.4 | 56.2 | 24.8 | Low concentration-low salinity polymer in situ rheology |
| NIL-16 | 22.0 | 118.9 | 56.5 | 24.4 | High concentration-high salinity polymer in situ rheology |

Table 1— Core properties of the Indiana limestone cores used in core flooding experiments

### Polymer solutions and brine.

Deionized (DI) water was used as the base for all synthetic brines. The DI water was obtained using a Millipore Sigma Milli-Q Direct water purification system that produces ultra-pure water directly from tap water through reverse osmosis. The DI water had a resistivity of 18.2 MΩ.cm. Three different synthetic brines, formation water, high salinity brine, and a 10-times diluted low salinity brine were formulated by dissolving weighted quantities of NaCl, $NaHCO_3$, anhydrous $Na_2SO_4$, $CaCl_2 \cdot 2H_2O$, and $MgCl_2 \cdot 6H_2O$ in DI water, with continuous magnetic stirring until complete dissolution. The resulting ion compositions and TDS values of different brines are summarized in Table 2. For higher salinities, vacuum filtering was conducted (Buchner funnel, Whatman grade 42, 2.5 μm). Light dead crude oil provided by Aramco was used. The density of the oil at 25°C was 0.87 g/cm3, and its viscosity at 25°C, 75°C and 95°C was 12.73 cP, 3.6 cP, and 2.76, respectively. The oil was mechanically filtered through Swagelok inline filters (0.5 and 2 μm). SARA (oil content) fractions in weight % were measured to be 22.3% saturates, 24.3% aromatics, 30.1% resins, and 23.3% asphaltenes. We prepared different glycerin solutions in 57670 ppm of high salinity brine. The goal was to obtain a concentration of glycerin solution that would have a similar Newtonian viscosity as that of low concentration-low salinity and high concentration-high salinity polymer solutions measured at 75 °C. It was found that a 96% glycerin solution prepared in the high salinity brine of 57670 ppm showed a similar Newtonian viscosity to the polymer solutions of low concentration-low salinity and high concentration-high salinity. The glycerin solution had a Newtonian viscosity of 27.2 cP at 75 °C and 13.3 cP at 95 °C.

The polymer used was a synthetic copolymer of acrylamide (AM) and 2-acrylamido-2-methylpropane sulfonic acid (AMPS) and it had a high molecular weight (Mw) of 8 million Dalton. The polymer, AN-125 SH, used is in powder form. The polymer was chosen due to the following reasons (a) Because of proven stability at relevant conditions of high temperature and high salinity reported by Jouenne (2020). (b) Its Mw is sufficient enough to generate viscoelasticity but not very high to minimize mechanical entrapment and pore plugging. The weighted polymer powder was slowly added to a strongly agitated brine vortex (high-speed mixing >500 rpm) for

dispersion at around 10 minutes. Then, low shear hydration (~250 rpm) was done for 24 hours to achieve full dissolution and hydration. Beakers were covered with aluminum foil throughout the solution preparation step to limit oxygen exposure. The polymer solutions were prepared in low salinity 5767 ppm brine and high salinity 57670 ppm brines with various concentrations of AN-125 SH ranging from 1000-10000 ppm.

| Ions | Formation water, ppm | High salinity brine, ppm | Low salinity brine, ppm |
|---|---|---|---|
| Sodium $Na^{+1}$ | 59,491 | 18,300 | 1,830 |
| Calcium $Ca^{+2}$ | 19,040 | 650 | 65 |
| Magnesium $Mg^{+2}$ | 2,439 | 2,110 | 211 |
| Sulfate $SO^{-2}$ | 350 | 4,290 | 429 |
| Chloride $Cl^{-1}$ | 132,060 | 32,220 | 3,220 |
| Bicarbonate $HCO^{-1}$ | 354 | 120 | 12 |
| TDS: | 213,734 | 57,670 | 5,767 |

Table 2—Formulated synthetic brine salt compositions used

**Polymer rheology measurements**

The bulk rheology (steady shear) tests were conducted on the polymer solutions with varying concentrations from 1000-10000 ppm in both low salinity 5767 ppm and high salinity 57670 ppm brines. The rheometer used was Anton Paar MCR 702 twin-drive with a concentric-cylinder geometry. The cup had an inner diameter of 28.91 mm that accommodated 20 ml sample volume, and the bob had a diameter of 26.66 mm with an effective length of 40 mm. Temperature was controlled at 75°C using the rheometer's Peltier system. A logarithmic shear rate sweep from 0.01 to 1000 s-1 was run using 30 measurement points with 1 min acquisition at each point. Measurements were initially planned at 95°C, such that we could have a comparison between the Newtonian viscosities of both the low and high salinity solutions, but equipment limitations didn't support this; thus, the steady shear rheology was conducted at 75°C and later supplemented by porous media single-phase polymer floods (in situ rheology).

**Contact angle and IFT measurements**

Static contact angle measurements were conducted to quantify the wettability changes of carbonate rock with different aqueous and polymer solutions. The Indiana limestone core was cut into ~ 1-cm x 1-cm chips and initially conditioned in formation brine to represent reservoir brine exposure. Contact angles were measured at ambient temperature using a drop shape analyzer in a captive-bubble configuration: a crude oil droplet was placed against a submerged rock surface while the chip remained immersed in the test aqueous phase, and the contact angle was determined through the aqueous phase. Two measurement phases were conducted: (a) pre-aging, where formation brine-saturated chips were tested in DI water, low salinity brine and high salinity brine. (b) post-aging, where chips were aged in light crude oil at 95°C for ~ 21 days. For example, Al-Ameer et al. (2023) recommended aging carbonate core samples for at least 14 days at 60°C to achieve oil-wet conditions. The chips were lightly wiped to remove the free surface oil without disturbing adsorbed films, and then re-tested in the surrounding brines and polymer solutions. The contact angle evolution across the phases showed a wettability shift from initially water-wet conditions towards strongly oil-wet behavior after crude oil aging. This will enable subsequent interpretation of polymer/brine effects on wettability in the core flooding experiments. IFT measurements were conducted using a spinning drop tensiometer with different combinations of brines and polymer solutions measured against the light crude oil at 95°C. These values of IFT were used in the computation of capillary numbers for CDC generation.

**Core flood experiments**

All flooding experiments were carried out at a constant rate using the core flooding setup shown in Fig. 1, with injection controlled by dual Teledyne ISCO syringe pumps. The accumulators contained the injection fluids, an oven set at a temperature of 95°C contained the Hassler core holder with a confining pressure set at 1700 psi, the inlet and outlet were connected to two separate pressure transducers, and a differential pressure transducer across the inlet and outlet with a range of 0-435 psi with an accuracy of ~ 0.065%. This accuracy allows measurement of up to 0.28 psi. The outlet was connected to a back pressure regulator that was set at 500 psi. Pressure data from the transducers were monitored continuously at each flux via the system's data acquisition software, and produced fluids were collected and measured downstream.

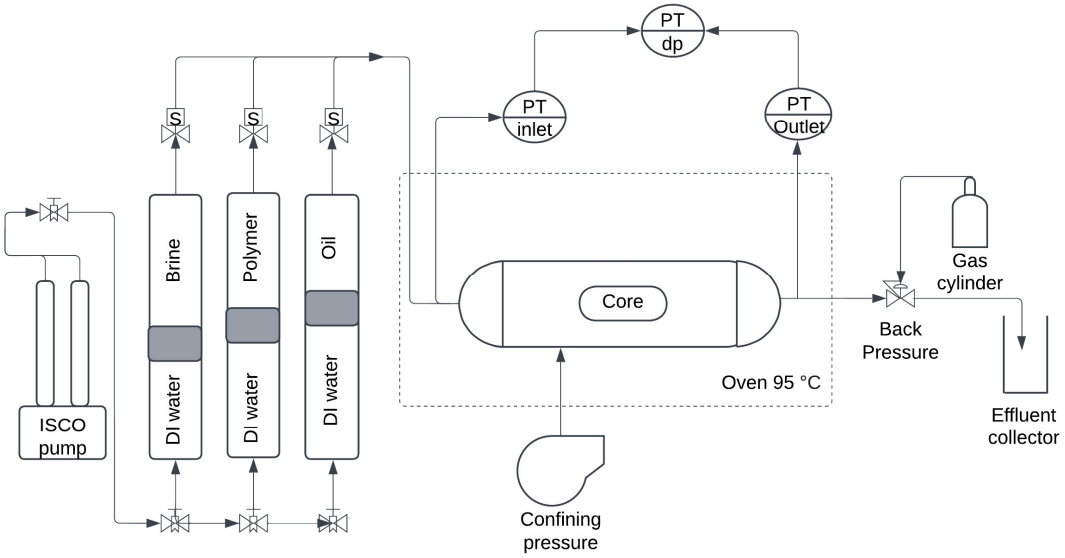


**Fig. 1—Schematic of the core flooding setup used for all core flood experiments**

To characterize the polymer solutions' behavior in porous media, single-phase in situ rheology experiments were conducted using the composite cores NIL-15 and NIL-16, having comparable porosity and permeability values shown in Table 1. These cores were initially fully saturated with formation salinity. The selected low and high-salinity polymer solutions were injected into the core NIL-15 and NIL-16, respectively. The flooding was at constant flux rates spanning 0.05-100 ft/day at each imposed rate 2.5-4.0 pore volumes (PV) were injected and stabilized pressure drop was recorded. Apparent viscosity was computed at each flux rate using Darcy's law assuming single-phase aqueous flow. The resulting apparent viscosity against flux rates trend was used to identify Newtonian regime, shear thinning behavior, potential onset of shear thickening, and indication of mechanical degradation during porous media flow.

The CDC curve generation oil desaturation experiments were conducted for both low salinity-low concentration (2500 ppm AN 125 SH in 5767 ppm brine) and high salinity-high concentration (4000 ppm AN 125 SH in 57670 ppm). The choice of salinity was to have a high salinity at 57670 ppm TDS representing typical injection water salinity and a low salinity was its 10 times dilution at 5767 ppm TDS. A similar low salinity water of 6898 ppm TDS was reported to yield higher wettability altering potential (AlSofi et al. 2018). The concentration for low salinity and high salinity polymers were obtained by performing bulk rheological experiments at 75°C to achieve similar Newtonian viscosities. In-situ rheology also confirmed their similar Newtonian viscosities. Indiana limestone cores NIL-06 and NIL-09 with permeability values of 110.9 md and 104.8 md, with porosity values of 23.7% and 22.7%, respectively, were used to conduct these experiments. These data indicate that the cores have similar petrophysical properties. The formation water saturated cores were oil flooded to establish the original oil in place (OIIP). Light crude oil was injected at 0.5 $cm^3$/min and injection continued for approximately 3 PV followed by an additional 3 PV until pressure drop stabilized. At this stabilized condition, only oil was the flowing phase with no water observed in the effluent. The recorded displaced brine volume collected in the effluent was used to compute initial oil saturation (Soi) and irreducible water saturation (Swi). At 95°C, the oil viscosity is 2.76 cP. The cores were next aged in crude oil at 75°C for 21 days to establish oil-wet conditions before secondary bump water flooding and tertiary flooding using glycerin and polymer flood with low and high-salinity polymer solutions. The oil-wet cores were placed in the core holder, and experimental conditions, including a confining pressure of 1700 psi, a back pressure of 500 psi, and a temperature of 95°C were established. Bump water flooding for both cores using high salinity brine was performed at Darcy flux rates 2-64 ft/day injecting 4.0-5.0 PV at each rate step until oil production ceased as characterized by stabilized pressure drops. This point marked a well-swept water-flooded residual oil. A 96% glycerin solution was injected to ensure any bypassed mobile oil was recovered. The flux rate was 0.05 ft/day and 2.5-3.0 PV were injected until only glycerin was the recovered phase and the pressure drop stabilized. Polymer flooding was then commenced by injection of 2500 ppm 5767 ppm low salinity solution into core NIL-06 and 4000 ppm 57670 ppm high salinity into core NIL-09. The polymer flooding in both cores was carried out at flux rates spanning from 0.05 to 100 ft/day. At each rate step, injection continued until steady state was achieved marked by a stabilized pressure drop and cessation of oil production in the effluent. Typically, 4.0-5.0 PV were required per each rate step (this was reduced to 2.5-3.0 PV at lower rates to limit run times). Stabilized pressure values, oil recovered, and effluent volumes were recorded at each rate step.

**CDC development**

The measured IFT of high salinity brine, glycerin, low salinity-low concentration polymer, and high salinity-high concentration polymer with crude oil at 95°C were 10.66, 18.14, 11.14, and 10.97 dynes/cm, respectively; these values are almost similar in magnitude. Since the capillary number depends on differential pressure gradients, IFT, and permeability, IFT measurements were done. During polymer flooding, the Darcy flux was increased stepwise from 0.05-100 ft/day, and at each rate, the stabilized differential pressure (ΔP) across the core and the cumulative oil produced were recorded; the residual oil saturation corresponding to each rate step was determined from the total oil collected up to that point. The CDC was then constructed by plotting the calculated residual oil saturation versus the corresponding capillary number for each injection stage. The capillary number was computed using Eq (1). To compare the CDC for low salinity-low concentration against high salinity-high concentration, only the differential pressure gradient in the fluid system was the variable, having fixed similar petrophysical properties and IFTs in magnitude.

## Results and Discussion

Initially, we discuss the results from steady shear rheometry, single-phase in-situ rheology, and contact angle measurements. Then we present the results associated with the generation of CDC. It was also attempted to interpret the obtained core flood recovery results to examine if the polymer viscoelasticity can offer benefits for Sor reduction for the typical carbonate field conditions and spacings. Finally, we shed insights on why wettability alteration and the onset of shear thickening is not sufficient for inducing higher Sor reduction during viscoelastic polymer flooding at the harsh carbonate conditions.

### Steady shear rheometry

A steady shear rheogram for AN-125 SH polymer obtained at a temperature of 75 °C and series of concentrations from 1000 to 10000 ppm, for both low and high salinity polymer solutions, is shown in Fig. 2a and Fig. 2b. The general trend is that for both the salinities, the increase in concentration led to the increase in Newtonian viscosity and an early onset of shear thinning and a late or similar onset of shear thickening. Our observation is consistent with the earlier reported findings (Azad 2024; 2023; Howe et al. 2015). Upon examining the effect of salinity as expected it is clear that the polymer solution's viscosifying ability decreases at each concentration at high salinity compared to low salinity. Our aim was to formulate and use two polymer solutions, one with low salinity and the other with high salinity at certain concentrations that give a similar Newtonian viscosity but differ in linear and non-linear viscoelasticity. It was found that 2500 ppm AN-125 SH in 5767 ppm low salinity brine and 4000 ppm AN-125 SH in high salinity brine polymer solutions showed comparable Newtonian viscosities of 27.8 cP and 26.5 cP, respectively, as shown in Fig. 2c. These two polymer solutions one with low concentration- low salinity and the other with high concentration-high salinity were chosen for our study.

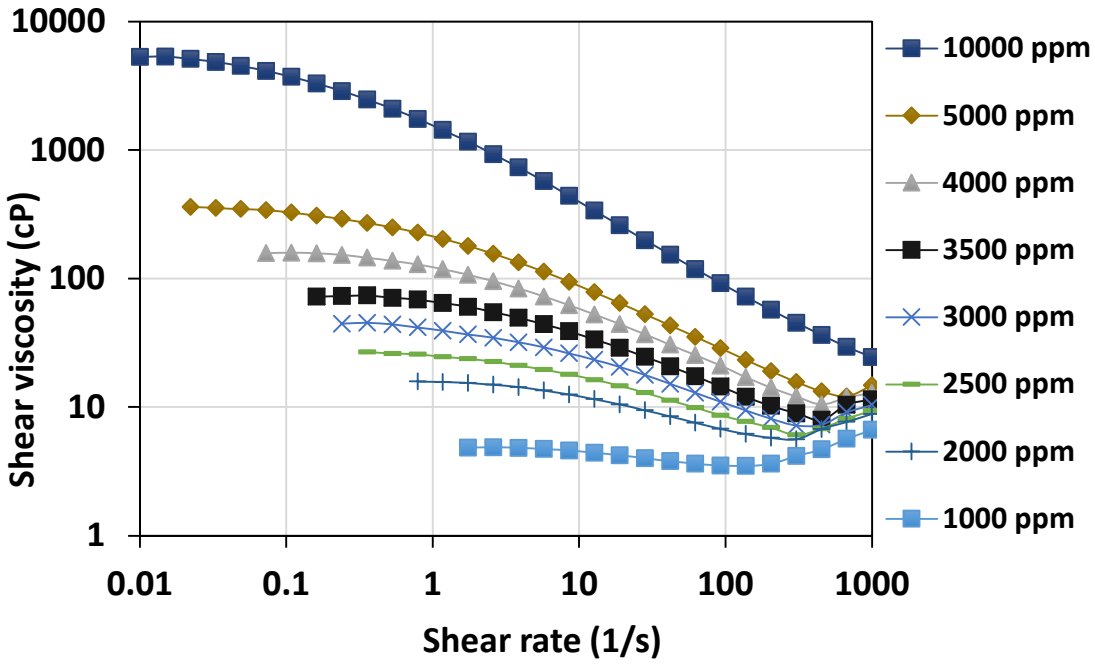


**Fig. 2a—Steady shear viscosity profile for various concentrations of AN-125 SH in 5767 ppm low salinity brine at 75°C**

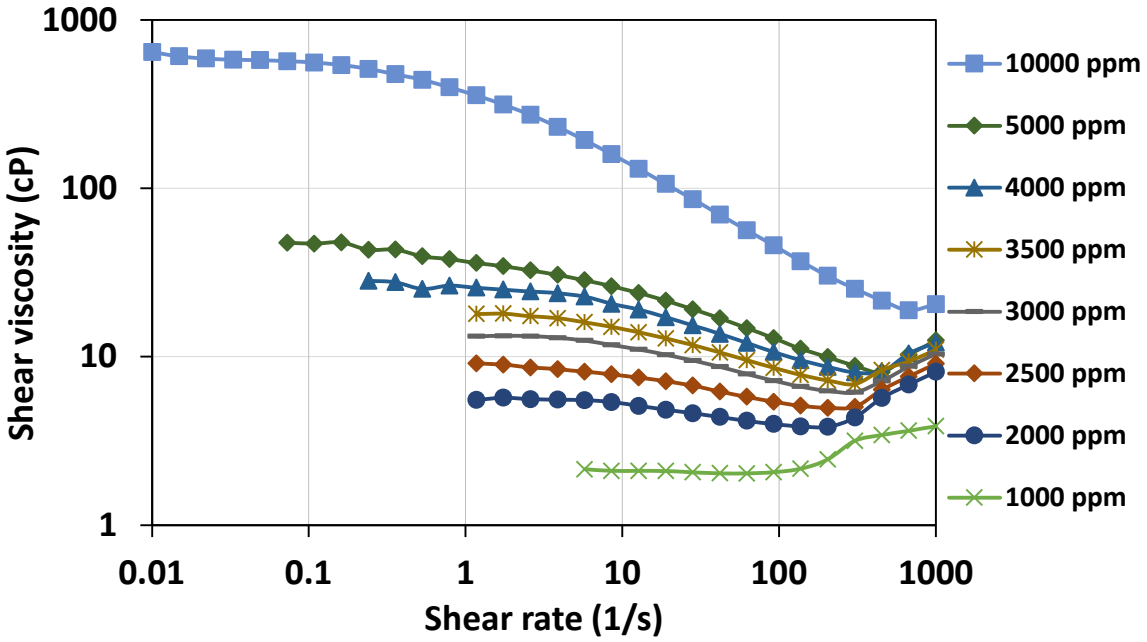


**Fig. 2b—Steady shear viscosity profile for various concentrations of AN-125 SH in 57670 ppm high salinity brine at 75°C**

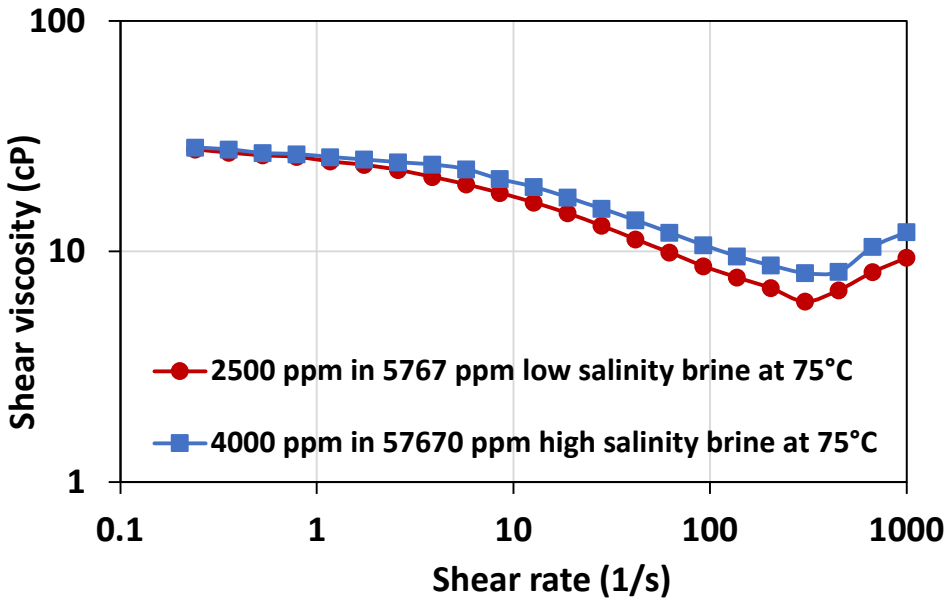


**Fig. 2c—Steady shear rheology for 2,500 ppm AN-125 SH in 5767 ppm low salinity brine and 4,000 ppm AN-125 SH in 57670 ppm high salinity brine solutions at 75°C**

### Contact angle measurements

Considering the importance of wettability for polymer flooding studies, contact angle measurements were performed. Contact angle is the measure of the wettability of surfaces. Contact angle measurements on rock oil/water phase systems provide one approach to measuring rock wettability (Morrow 1990). Rock surfaces are classified as water-wet, neutral-wet, or oil-wet when the water contact angle is in the range of 0 to 75, 75 to 105, and 105 to 180° (Anderson 1986). The contact angles of different aqueous solutions/oil systems on rock chips are measured through the aqueous phase (water) to quantify the wettability-altering potential. The Indiana limestone core chips we used in the contact angle measurements are similar to the cores used in core flooding experiments to mimic similar conditions. The initial contact angle measurement with DI water showed a value of 15.7°. For measurements with low salinity brines, the contact angle was 15.4°, and for high salinity, it was 15.7°. Upon aging the core chips in crude oil for a duration of 21 days, the rock surface became extremely oil wet with contact angles of 167.6° and 172.8° when measured in low salinity and high salinity

brine, respectively. The changes in contact angles at different stages are shown in Fig. 2(a) and (b). When the polymer was used in contact angle measurements, it was found that there was no significant impact of the polymer on the wettability-altering potential even at low salinity. Nevertheless, the low salinity polymer showed relatively better wettability altering potential when compared with the high salinity polymer, with contact angles of 165.5° and 170.4° respectively, which is consistent with the literature (Li et al. 2020; AlSofi et al. 2018). These results will be used during the later interpretation of the CDC curves.

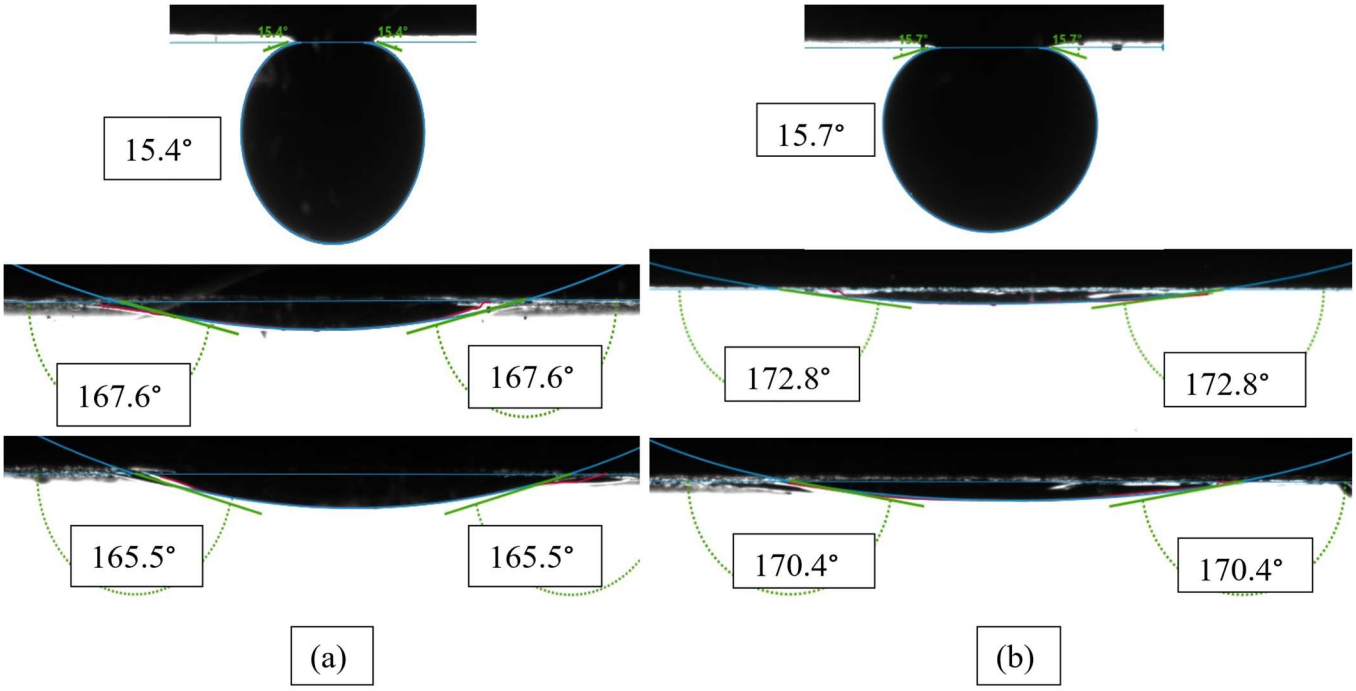


**Fig. 2—(a) Contact angle (from top) with pre-aged chips measured in low salinity brine, post aging in oil measured in low salinity brine and bottom measured in 2500 ppm in 5767 ppm low salinity brine polymer solution (b) Contact angle (from top) with pre-aged chips measured in high salinity brine, post aging in oil measured in high salinity brine and bottom measured in 4000 ppm in 57670 ppm high salinity brine polymer solution.**

### Single-phase (in situ) rheology

The increase in salinity will lead to a decrease in the apparent viscosity of the polymer flood. As mentioned, we intend to optimize the concentration of polymer for the two salinities such that their Newtonian viscosities remain similar during core flooding experiments conducted for CDC generation. Since the increase in salinity leads to a reduction of apparent viscosity and an increase in concentration leads to an increase in apparent viscosity, we found that the 2500 ppm low salinity and 4000 ppm high salinity led to similar Newtonian viscosity based on the steady shear rheology shown in Fig. 2c at a temperature of 75 °C. We could not perform the steady shear rheology experiments at our temperature of interest, which is 95°C, but in situ rheological experiments were carried out at 95 °C with Indiana limestone cores to verify obtaining similar Newtonian viscosities for the two polymer solutions. The purpose of obtaining the Newtonian viscosity is more relevant for the field projects since these viscosities are going to be experienced as the polymer flood moves far away from the wellbore (Azad and Seright 2025). Besides that, in situ rheology also provides information about the various flow regimes encountered by the polymer solution in porous media.

The generated in situ rheograms for the low and high-salinity polymer solutions are shown in Fig. 3.

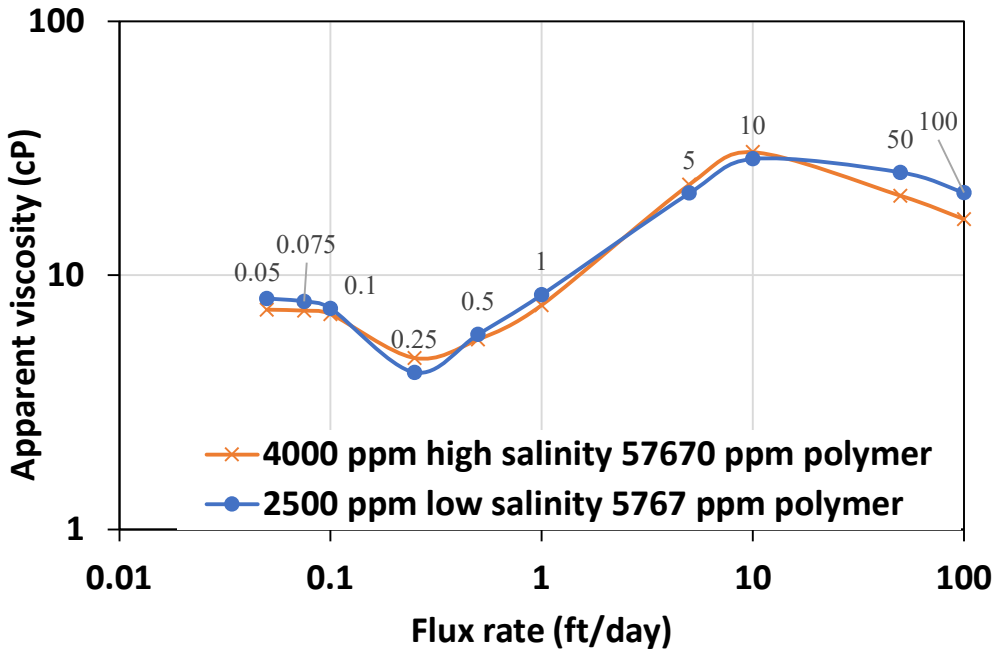


**Fig. 3—In situ rheograms of 2500 ppm AN-125 SH in 5767 ppm low salinity brine and 4000 ppm AN-125 SH in 57670 ppm high salinity brine.**

According to the literature, four distinct flow regimes are evident for viscoelastic polymer solutions: Newtonian, shear thinning, shear thickening, and mechanical degradation. For both low and high salinity polymer solutions, the onset of shear thickening is evident indicating that they are viscoelastic. Further, both the polymer solutions, the onset of shear thinning, shear thickening, and mechanical degradation are similar. However, the higher magnitude of mechanical degradation is associated with high salinity-high concentration polymer solution when compared to low salinity-low concentration polymer solution, which is consistent with the previously reported findings (Zaitoun et al. 2012; Azad 2023; Seright et al. 2023,2025). It is evident from Fig. 3 that the apparent viscosities in the Newtonian and shear thickening regimes are quite similar for low salinity-low concentration and high salinity-high concentration polymer solutions. We will be using these apparent viscosities for further interpretation and discussion of our core flood experiment results in the following sections.

**CDC generation**

To generate the CDC and evaluate the oil desaturation potential of low-salinity-low-concentration and high-salinity-high-concentration polymer systems, we conducted constant-rate core flooding oil desaturation experiments. The cores used were NIL-06 and NIL-09, which had similar petrophysical properties as shown in Table 1. Both cores were subjected to a high salinity bump water flood from 2 to 64 ft/day to achieve well-swept residual oil. The low salinity and high salinity polymers showed a similar onset of shear thickening at around 0.25 ft/day. The glycerin flood was conducted at a flux rate 0.05 ft/day to eliminate if any bypassed oil within the cores. Afterwards, the core NIL-06 was flooded with 2500 ppm AN-125 SH in low salinity 5767 ppm brine, and NIL-09 was flooded with 4000 ppm AN-125 SH in high salinity 57670 ppm brine. At 2 ft/day water flood majority of the oil was recovered from the core, with recovery factor of 47.6% from NIL-06 and that of 49.2% from NIL-09. Overall, the water flooding recovery rates from the bump rates of 2-64 ft/day had comparable recoveries of 48.7% and 49.8% from NIL-06 and NIL-09, respectively. The glycerin flood from these two cores had no measurable oil recovery, except traces of droplets from the effluents. For polymer floods in both cores at flux rates of 0.05 to 1 ft/day, there was no oil recovery from the cores; this is seen as a plateau in Fig. 5a and Fig. 6a where oil saturation within the core did not change even though the onset of shear thickening for the two polymer solutions was around 0.25 ft/day. This observation is in contradiction to the concept that the onset of shear thickening can induce Sor reduction. The pressure gradients measured at 1 ft/day were 32.4 psi/ft and 28.3 psi/ft for 2500 ppm low salinity and 4000 ppm high salinity polymer solutions, respectively. The choice of using oil desaturation curves to represent recoveries rather than recovery factor plots is to have a similar kind of comparison to the CDC curves since both are plotted with oil saturation on one axis. For the details on recovery factors and pressure drop gradients values obtained with water flooding, glycerin flooding and polymer flooding in the two desaturation experiments, refer to Table A-1and Table A-2 in the appendix. The measured pressure gradient for the two polymer solutions can be seen in Fig. 5b and Fig. 6b. From the figures, it is observed that for the two cores of NIL-06 and NIL-09, the last water flood rate at 64 ft/day generated pressure gradients of ~100.0 psi/ft and 113.2 psi/ft, respectively. These two values are still greater than the pressure gradients generated by the polymer solutions when flooded at flux rates from 0.05 to 1 ft/day. This means a very high capillary number is imposed during water flooding to make the residual oil highly discontinuous and trapped. The first oil during polymer flooding was recovered at 5 ft/day with an incremental

recovery factor (IRF) of 1.0% using the low salinity polymer solutions, while for the high salinity polymer solution at the same rate had an IRF of 0.8%, with pressure gradients of 179.89 psi/ft and 225.75 psi/ft, respectively. The capillary numbers at these conditions for both low and high-salinity polymers were $4.0x10^{-5}$ and $4.82x10^{-5}$, respectively. Upon increasing the rates for both polymer floods to 10, 50, and 100 ft/day, more oil was recovered with total IRF of 12.5% and 10.6% for low salinity polymer and high salinity polymer, respectively. The curves showing the overall trends of IRF and stable pressure drop gradients obtained with low salinity and high salinity polymer solutions are presented in Fig. 4. It is evident that the high salinity polymer generated higher pressure gradient from 5 ft/day to 100 ft/day than low salinity polymer flood, even though the high salinity polymer exhibited a higher magnitude of mechanical degradation at rates of 50 and 100 ft/day in the in situ rheograms seen earlier (Fig. 3).

CDCs generated for two polymer solutions were provided in Fig. 5. It becomes clear that the two curves do not overlap initially, this is due to difference in Sor after water flooding which was 0.31 for low salinity polymer flood and 0.28 for high salinity polymer flood. The IFT measured at 95°C of the two systems, oil/low salinity polymer and oil/high salinity polymer were 11.14, and 10.97 dynes/cm, respectively. These IFT values were similar in magnitude between the two systems. The only variable in computing the capillary number was the generated pressure gradients. The critical capillary number marking the onset for rapid oil mobilization was determined to be $4.0x10^{-5}$ and $4.82x10^{-5}$ for the low and high salinity polymer floods, respectively.

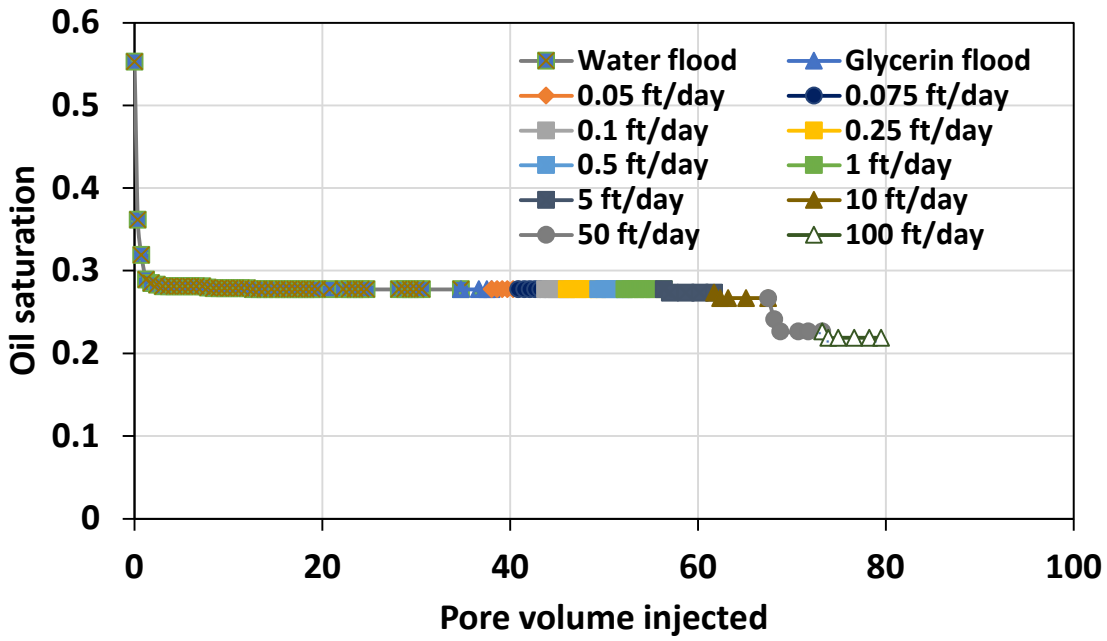


**Fig. 5a—Oil desaturation for NIL-09 core showing contributions from waterflooding, glycerin, and 4000 ppm AN-125 SH in 57670 ppm high salinity brine polymer flooding stages**

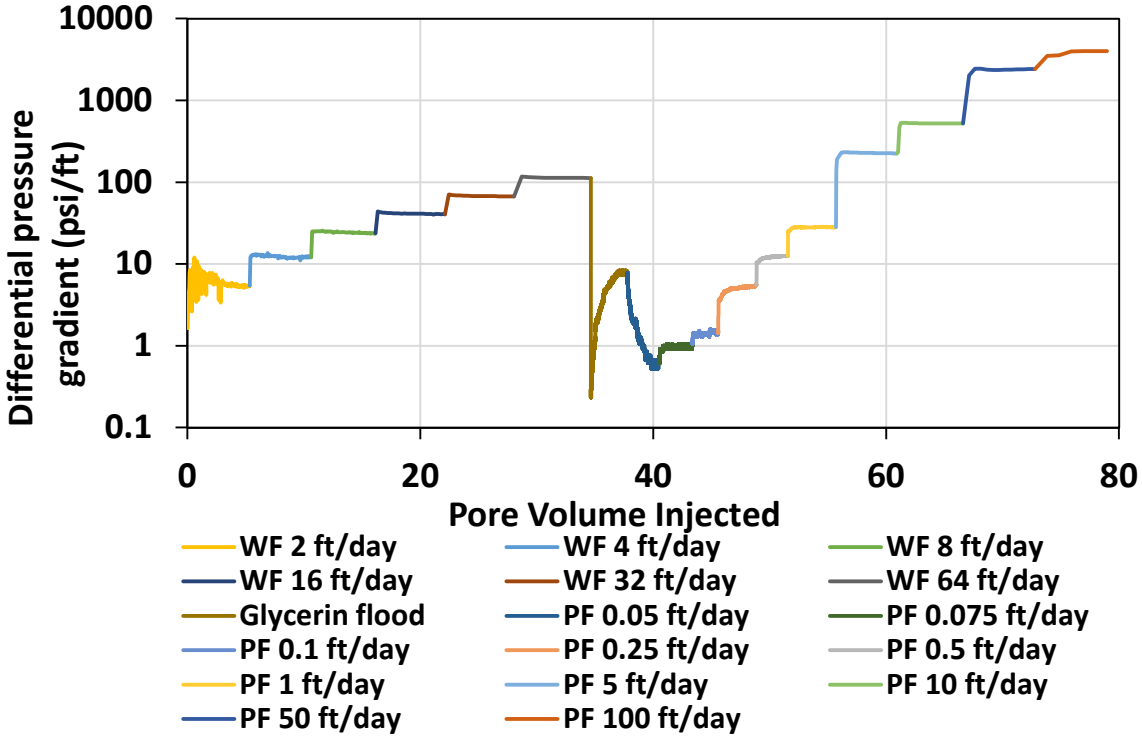


**Fig. 5b—Differential pressure gradient profile during waterflooding, glycerin flooding, and 4000 ppm AN-125 SH in 57670 ppm high salinity brine polymer flooding on a semi-log scale**

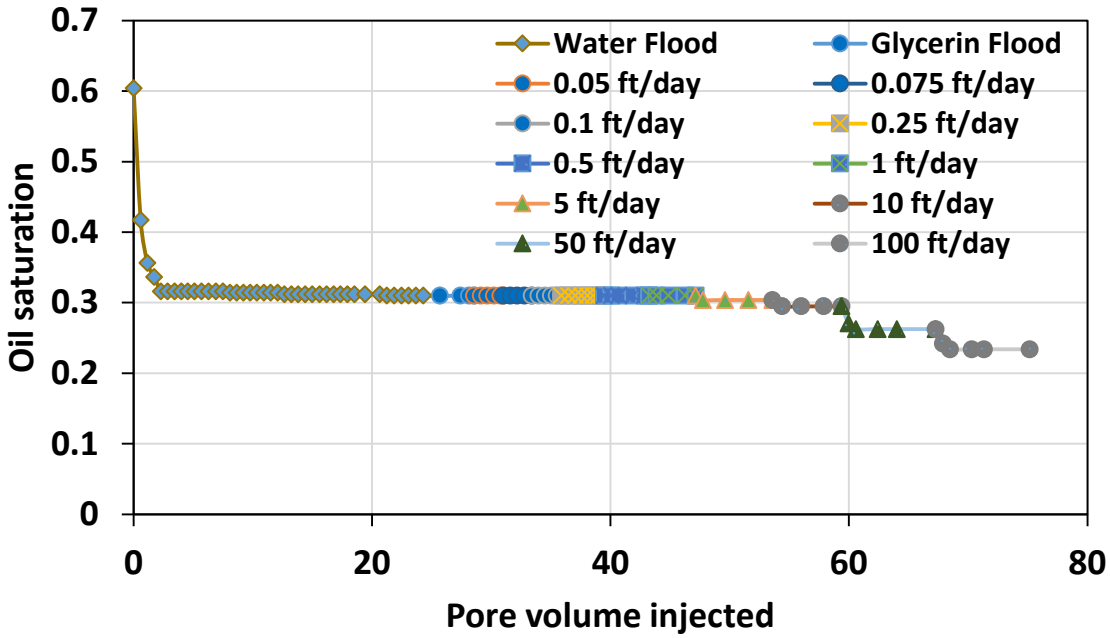


**Fig. 6a—Oil desaturation for NIL-06 core showing contributions from waterflooding, glycerin, and 2500 ppm AN-125 SH in 5767 ppm low salinity brine polymer flooding stages**

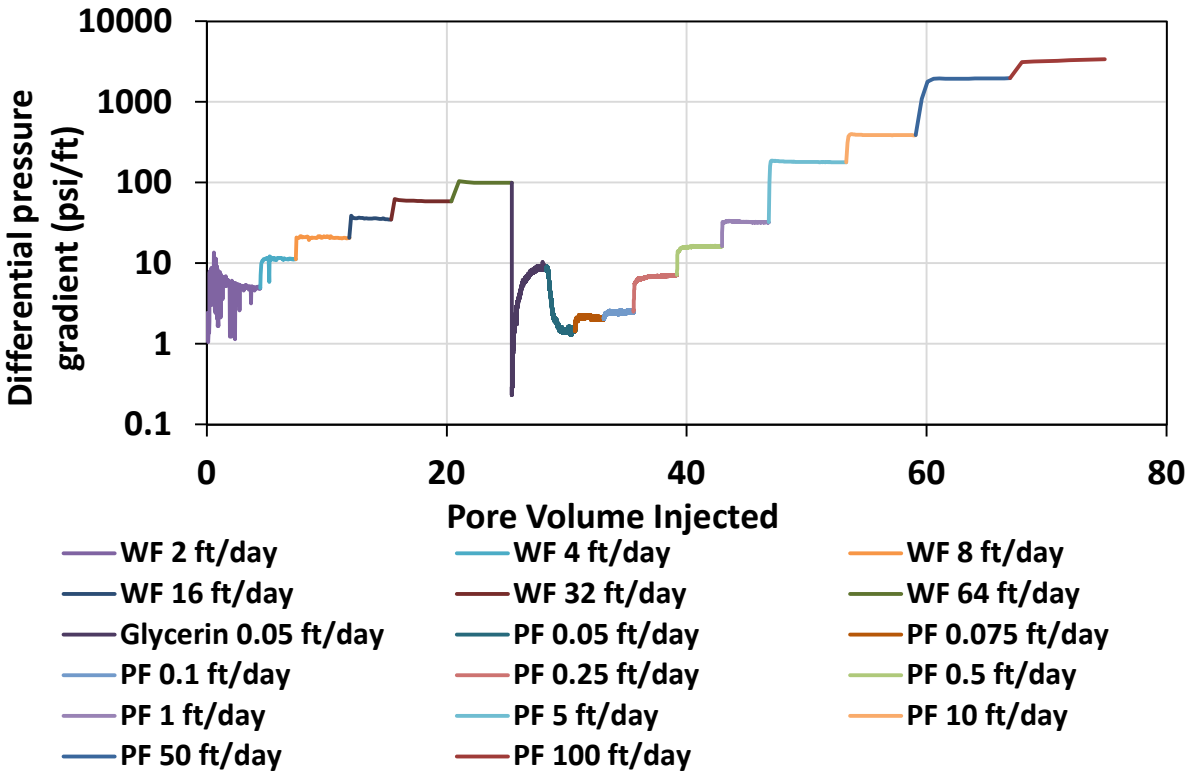


**Fig. 6b—Differential pressure gradient profile during waterflooding, glycerin flooding, and 2500 ppm AN-125 SH in 5767 ppm low salinity brine polymer flooding on a semi-log scale**

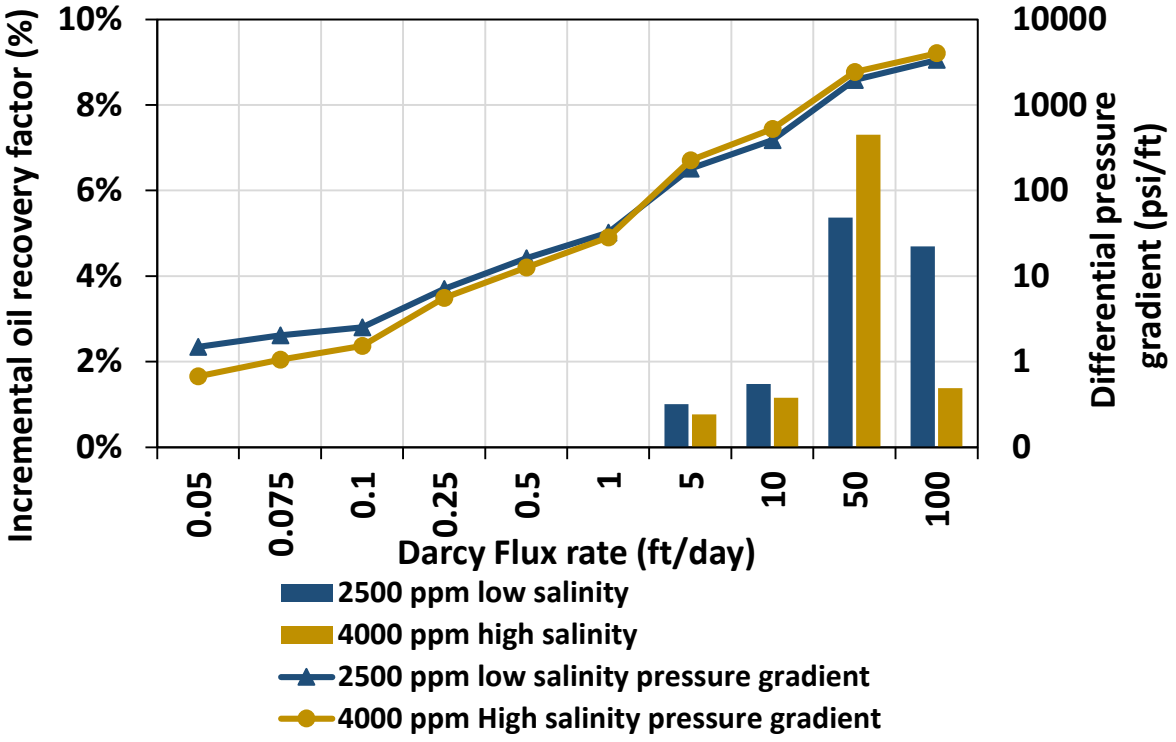


**Fig. 4—Comparative plot for 2500 ppm AN-125 SH in 5767 ppm low salinity brine and 4000 ppm AN-125 SH in 57670 ppm high salinity brine polymer solutions with stable pressure drop gradients, and incremental recoveries at various flux rates**

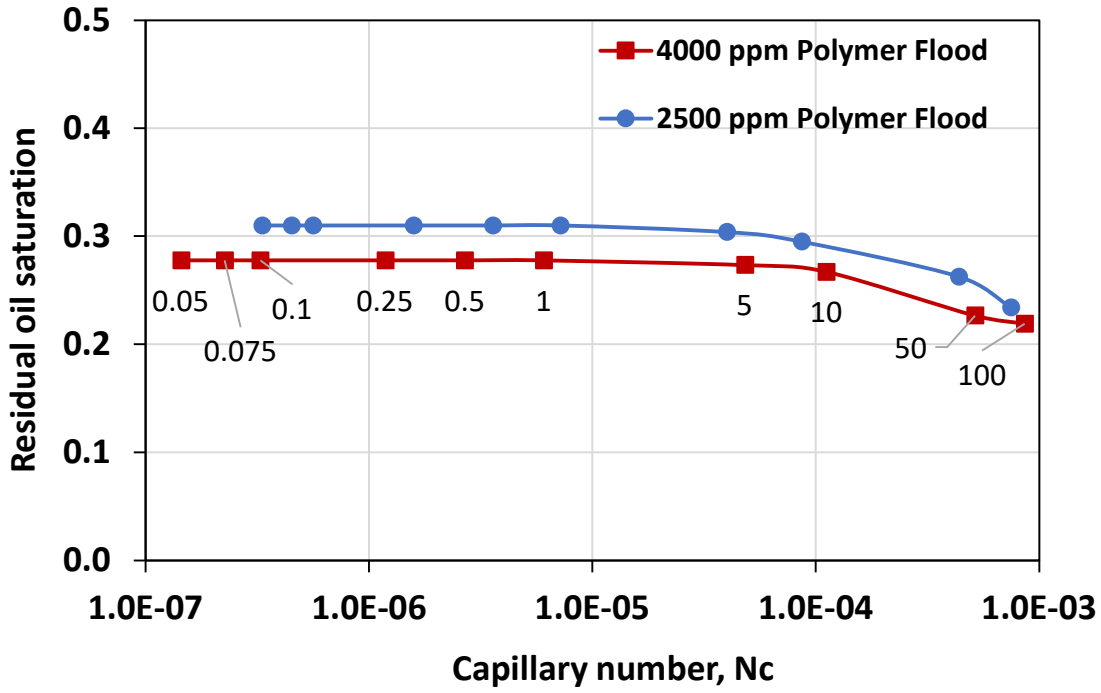


**Fig. 5—CDC generated for 2500 ppm AN-125 SH in 5767 ppm low salinity brine and 4000 ppm AN-125 SH in 57670 ppm high salinity brine polymer floods**

**Laboratory Sor reduction by low and high salinity viscoelastic polymer injection**

For low flux rates from 0.05 ft/day to 1 ft/day, both low and high salinity polymers don't reduce Sor further. This is despite the fact that both the polymer solutions started showing shear thickening at the flux rate of 0.25 ft/day (Fig. 3). At 5 ft/day, both polymer solutions show a reduction in Sor. The critical capillary number is also a bit lower for low salinity polymer solution when compared to high salinity polymer solutions (Table A-1 and Table A-2). Increasing the flux rate further up to 100 ft/day, additional desaturation is happening for both polymer solutions, yielding slightly higher incremental residual oil recovery of 12.5% with low salinity in contrast to 10.6% obtained with high salinity polymer solution (Table A-1 and Table A-2). This result in interesting despite the low salinity-low concentration polymer solution generating a relatively lower pressure gradient than high salinity-high concentration polymer solution (Fig. 4). The ability of low salinity polymer solutions to induce slightly higher oil recovery when compared to high salinity polymer at relatively lower pressure gradient may be due to the relatively better wettability alteration potential associated with low salinity polymer. Does that mean the low-salinity polymer's wettability alteration guarantees a considerable Sor reduction in the studied carbonate conditions of interest? This point is discussed in the next section.

**Can the chosen polymer solutions be expected to contribute to Sor reduction in high-temperature, high-salinity, extremely oil-wet carbonate reservoirs?**

A flux rate of 5 ft/day is required to induce Sor reduction in both the cores (Table A-1 and Table A-2). Azad and Seright (2025) analyzed polymer flood projects across nine different countries, calculated the average velocity of propagating polymer solutions, and examined the radial distance that the specific flux can reach for many of those projects. In this section, we compare our lab results with some of the polymer flood projects analyzed by Azad and Seright (2025). Initially, we compare our observation with the polymer flood projects developed using vertical wells. 5 ft/day is relatively a higher flux that can cover less than 10 ft for the injection rate of 175 STB/D and 335 STB/D for an average thickness of 20 ft reservoir (Please see Figure 11a in SPE 223155-PA). If the reservoir is highly permeable (which is not the case with most Middle East carbonates), then higher injection could be opted. In the Marmul field, an injection rate of 3145 STB/D was imposed. Even then, 5 ft/day can extend to a 10 ft radius (Figure 12 of SPE 223155-PA). The low thickness can amplify the average velocity. We considered the case of the Diadema project, where the low thickness of 13.12 ft was applied. In this case, a 5 ft/day average velocity can extend to around 50 ft (Figure 13a of SPE 223155-PA). For the average thickness, these values drop to 30 ft. An interwell spacing of such distance will not be realistic for field projects, so this analysis clearly indicates that these polymer solutions cannot reduce Sor in a significant portion of the harsh carbonate conditions.

**Why is wettability alteration and the onset of shear thickening alone not sufficient for inducing rapid oil mobilization in the studied conditions?**

The analysis made in the previous paragraph also implies that even though a wettability-altering is occurring for the low salinity polymer solutions, these effects by themselves cannot mobilize the discontinuous residual oil at field-relevant fluxes of 0.05 ft/day and around. One may wonder that the low salinity polymer solutions were reported to induce spontaneous imbibition oil recovery from oil-wet carbonates by around 30% (Figure 8 of SPE 208581-PA). Note that Souayeh et al. (2022) didn't use the cores that were subjected to bump flooding as we did. Bump flooding to a higher rate leads to discontinuous oil with strong trapping pressure. To overcome such trapping in extreme oil-wetting conditions of 172.8°, the wettability alteration alone doesn't suffice, and rather, a high-flux needs to be synergized with it to induce Sor reduction. Moreover, a careful look into Fig. 3 indicates that the onset of shear thickening occurs around the flux rate of 0.25 ft/day with low salinity polymer injection, and yet 5 ft/day is required to induce Sor reduction. This signifies that trapping is high enough that the shear thickening onset alone is not sufficient to reduce Sor. Instead, a higher flux in the shear thickening regime is required to induce Sor reduction in the studied conditions. To summarize, a strong wetting nature, coupled with the presence of highly discontinuous, capillary-trapped, well-swept residual oil in the oil-wet pores at high temperature conditions, necessitates a relatively higher flux to induce Sor reduction in the lab experiments.

## Conclusions

Two viscoelastic polymer solutions prepared with different concentrations and salinity were examined to evaluate their Sor reduction capability in harsh, oil-wetting carbonate reservoirs. Two CDC curves were generated and the results were interpreted to examine the potential of these polymer solutions to induce Sor reduction in the field.

1. The shear thickening onset rate is 0.25 ft/day for both low and high salinity viscoelastic polymer solutions in the studied media. The in-situ apparent viscosity is similar for both polymer solutions. The shear thinning onset and onset velocity of mechanical degradation were also similar for both polymer solutions.

2. Although 0.25 ft/day is the onset rate for shear thickening, the flux rate of 5 ft/day is required to induce significant Sor reduction from oil-wet carbonate cores having highly discontinuous oil in the lab.

3. The critical capillary number (Nc) in both the floods corresponding to 5 ft/day are $4.0 \times 10^{-5}$ and $4.82 \times 10^{-5}$ for low salinity and high salinity viscoelastic polymer solutions, respectively.

4. An important learning is that the onset of shear thickening doesn't guarantee significant Sor reduction or make the critical capillary number lower in oil wet carbonates.

5. Translation of rapid oil mobilization velocity (5 ft/day) for the typical field settings indicates the shear thickening onset velocity cannot cover more than 10-50 ft of the radial distance. This is impractical considering the typically larger well spacings used in polymer flooding projects.

6. Neither the shear thickening onset nor slight wettability alterations offered by the low and high salinity polymer solutions guarantees Sor reduction in the lab that is beneficial for field applications.

7. The higher oil-wetting nature and highly discontinuous oil's presence impede its mobilization through relatively low flux which makes the carbonate rock unsuitable candidate to reap the benefits of Sor reduction from the injection of low and high salinity viscoelastic polymer solutions at least in the tertiary mode.

## Nomenclature

AM = acrylamide

AMPS = 2-acrylamido-2-methylpropane sulfonic acid

CDC = capillary desaturation curve

cEOR = chemical enhanced oil recovery

DI = deionized water

EOR = enhanced oil recovery

IFT = interfacial tension

IRF = incremental recovery factor (%)

Nc = capillary number (dimensionless)

OIIP = original oil in place

PV = pore volume

RF = recovery factor (%)

Soi = initial oil saturation

Sor = residual oil saturation

Swi = irreducible water saturation

TDS = total dissolved solids (ppm)


## Acknowledgements

We would like to acknowledge the funding received from Saudi Aramco for the project (CIPR 2359). We would like to express our sincere gratitude to SNF company for providing AN-125 polymers. Further, we are deeply thankful to King Fahd University of Petroleum and Minerals (KFUPM), the Center for Integrated Petroleum Research (CIPR) for providing us with access to their state-of-the-art laboratories and resources and the lab engineers (Ridha, Assad Barri, Ammar, Jafar Al Hamad) who assisted during performing these experiments.


## References


Abrams, A. 1975. "The Influence of Fluid Viscosity, Interfacial Tension, and Flow Velocity on Residual Oil Saturation Left by Waterflood." SPE Journal **15** (05): 437–47. https://doi.org/10.2118/5050-PA.

Al-Ameer, M. A., Azad, M. S., Al-Shehri, D. et al. 2023. "A Guide for Selection of Aging Time and Temperature for Wettability Alteration in Various Rock-Oil Systems." ACS Omega **8** (34): 30790–801. https://doi.org/10.1021/acsomega.3c00023.

Al-Amrie, O., Sophie P., Adrian P. et al. 2015. "The First Successful Chemical EOR Pilot in the UAE: One Spot Pilot in High Temperature, High Salinity Carbonate Reservoir." Paper presented at the Abu Dhabi International Petroleum Exhibition and Conference, Abu Dhabi, UAE, November. https://doi.org/10.2118/177514-MS.

Al-Saadi, F. S., Amri, B. A., Nofli, S. et al. 2012. "Polymer Flooding in a Large Field in South Oman-Initial Results and Future Plans." Paper presented at the SPE EOR Conference at Oil and Gas West Asia, Muscat, Oman, April. https://doi.org/10.2118/154665-MS.

AlSofi, A. M., Wang, J., AlBoqmi, A. M. et al. 2019. "Smartwater Synergy with Chemical Enhanced Oil Recovery: Polymer Effects on Smartwater". SPE Reservoir Evaluation & Engineering **22** (01): 61–77. https://doi.org/10.2118/184163-PA.

Amiri, M., Fatemi, M., and Biniaz, D. E. 2022. "Effect of Brine Salinity and Hydrolyzed Polyacrylamide Concentration on the Oil/Brine and Brine/ Rock Interactions: Implications on Enhanced Oil Recovery by Hybrid Low Salinity Polymer Flooding in Sandstones". Fuel **324**: 124630. https://doi. org/10.1016/j.fuel.2022.124630.

Anderson, W. 1986. "Wettability Literature Survey-Part 2: Wettability Measurement." Journal of Petroleum Technology **38** (11): 1246–1262.

Azad, M. S. and Trivedi, J. J. 2019a. "Novel Viscoelastic Model for Predicting the Synthetic Polymer's Viscoelastic Behavior in Porous Media Using Direct Extensional Rheological Measurements." Fuel **235**: 218–226. https://doi.org/10.1016/j.fuel.2018.06.030.

Azad, M. S. and Trivedi, J. J. 2019b. "Quantification of the Viscoelastic Effects During Polymer Flooding: A Critical Review". SPE Journal **24** (06): 2731–2757. https://doi.org/10.2118/195687-PA.

Azad, M. S. and Trivedi, J. J. 2020a. "Does Polymer's Viscoelasticity Influence Heavy-Oil Sweep Efficiency and Injectivity at 1 Ft/D?" SPE Reservoir Evaluation & Engineering **23** (02): 446–462. https://doi.org/10.2118/193771-PA.

Azad, M. S. and Trivedi, J. J. 2020b. "Extensional Effects during Viscoelastic Polymer Flooding: Understanding Unresolved Challenges." SPE Journal **25** (4): 1827–1841. https://doi.org/10.2118/201112-PA.

Azad, M. S. and Trivedi, J. J. 2021. “Quantification of Sor Reduction during Polymer Flooding Using Extensional Capillary Number.” SPE Journal. **26** (3): 1469–1498. https://doi.org/10.2118/204212-PA.

Azad, M. S. 2023. “Characterization of Nonlinear Viscoelastic Properties of Enhanced Oil Recovery Polymer Systems Using Steady-Shear Rheometry.” SPE Journal **28** (02): 664–682. https://doi.org/10.2118/212824-PA.

Azad, M. S. 2024. “Influence of Polymer Concentration on the Viscous and (Linear and Non-Linear) Viscoelastic Properties of Hydrolyzed Polyacrylamide Systems in Bulk Shear Field and Porous Media.” Polymers **16** (18) https://doi.org/10.3390/polym16182617.

Azad, M. S. and Seright, R. S. 2025. “Are Field Polymer Enhanced Oil Recovery Projects Reaping the Benefits of Residual Oil Saturation Reduction Due to Polymer Viscoelasticity?” SPE Journal **30** (06): 3792–3809. https://doi.org/10.2118/223155-PA.

Barri, A., Azad, M. S., Al-Shehri, D. et al. 2023. “Is There a Viscoelastic Effect of Low-MW HPAM Polymers on Residual Oil Mobilization in Low Permeability Rocks at a Darcy Velocity of 0.2 Ft/Day?” Energy Fuels **37** (14): 10188–10199. https://doi.org/10.1021/acs.energyfuels.3c00955.

Chatzis, I., Kuntamukkula, M. S., and Morrow, N. R. 1988. “Effect of Capillary Number on the Microstructure of Residual Oil in the Strongly Water-Wet Sandstones.” SPE Reservoir Engineering **3** (03): 902–912. https://doi.org/10.2118/13213-PA.

Chatzis, I. and Morrow, N. R. 1984. “Correlation of Capillary Number Relationships for Sandstone.” SPE Journal **24** (05): 555–562. https:// doi.org/10.2118/10114-PA.

Clarke, A., Howe, A. M., Mitchell, J. et al. 2016. “How Viscoelastic-Polymer Flooding Enhances Displacement Efficiency.” SPE Journal **21** (03): 0675–0687. https://doi.org/10.2118/174654-PA.

Dafaalla, M., Azad, M. S., Ayirala, S. et al. 2025. “Potential of Polymer’s Viscosity and Viscoelasticity for Accessible Oil Recovery during Low Salinity Polymer Flooding in Heterogeneous Carbonates.” Fuel **379**: 133008. https://doi.org/10.1016/j.fuel.2024.133008.

Delamaide, E., Bazin, B., Rousseau, D. et al. 2014. “Chemical EOR for Heavy Oil: The Canadian Experience.” March 31. Paper presented at the SPE EOR Conference at Oil and Gas West Asia, Muscat, Oman, March. https://doi.org/10.2118/169715-MS.

Delamaide, E., Zaitoun, A., Renard, G. et al. 2014. “Pelican Lake Field: First Successful Application of Polymer Flooding in a Heavy-Oil Reservoir.” SPE Reservoir Evaluation & Engineering **17** (03): 340–354. https://doi.org/10.2118/165234-PA.

Dombrowski, H. S., and Brownell, L. E. 1954. “Residual Equilibrium Saturation of Porous Media.” Industrial & Engineering Chemistry **46** (6): 1207–1219. https://doi.org/10.1021/ie50534a037.

Durst, F., Haas, R., and Interthal, W. 1987. “The Nature of Flows through Porous Media.” Journal of Non-Newtonian Fluid Mechanics **22** (2): 169–189. https://doi.org/10.1016/0377-0257(87)80034-4.

Ehrenfred, D. 2013. “Impact of Viscoelastic Polymer Flooding on Residual Oil Saturation in Sandstones.” MS Thesis, The University of Texas, Austin, Texas, USA. http://hdl.handle.net/2152/23870.

Green, D. and Willhite, P. 2018. “Enhanced Oil Recovery.” (Second Edition), Texas, USA: Textbook Series, Society of Petroleum Engineers. https://doi.org/10.2118/9781613994948.

Guo, H., Song, K., Liu, S. et al. 2021. “Recent Advances in Polymer Flooding in China: Lessons Learnt and Continuing Development.” SPE Journal. **26** (4): 2038–2052. https://doi.org/10.2118/204455-PA.

Howe, A. M., Clarke, A., and Giernalczyk, D. 2015. “Flow of Concentrated Viscoelastic Polymer Solutions in Porous Media: Effect of M(W) and Concentration on Elastic Turbulence Onset in Various Geometries.” Soft Matter **11** (32): 6419–6431. https://doi.org/10.1039/c5sm01042j.

Jouenne, S. 2020. “Polymer Flooding in High Temperature, High Salinity Conditions: Selection of Polymer Type and Polymer Chemistry, Thermal Stability.” Journal of Petroleum Science and Engineering **195**: 107545. https://doi.org/10.1016/j.petrol.2020.107545.

Jouenne, S., and Guillaume H. 2020. “Correlation of Mobility Reduction of HPAM Solutions at High Velocity in Porous Medium with Ex-Situ Measurements of Elasticity.” SPE Journal **25** (01): 465–480. https://doi.org/10.2118/198899-PA.

Koh, H., Lee, V. B., and Pope, G. A. 2018. “Experimental Investigation of the Effect of Polymers on Residual Oil Saturation.” SPE Journal **23** (01): 1–17. https://doi.org/10.2118/179683-PA.

Lee, Y., Lee, W., Jang, Y. et al. 2019. “Oil Recovery by Low-Salinity Polymer Flooding in Carbonate Oil Reservoirs.” Journal of Petroleum Science and Engineering **181**: 106211. https://doi.org/10.1016/j.petrol.2019.106211.

Li, Z., Ayirala, S., Mariath, R. et al. 2020. “Microscale Effects of Polymer on Wettability Alteration in Carbonates.” SPE Journal **25** (4): 1884–1894. https://doi.org/10.2118/200251-PA.

Li, Z., Xu, Z., Ayirala, S. et al. 2020. “Smartwater Effects on Wettability, Adhesion, and Oil Liberation in Carbonates.” SPE Journal **25** (04): 1771–1783. https://doi.org/10.2118/193196-PA.

Moe Soe Let, K. P., Manichand, R. N., and Seright, R. S. 2012. “Polymer Flooding a ~500-Cp Oil.” Paper presented at the SPE Improved Oil Recovery Symposium, Tulsa, Oklahoma, USA, April. https://dx.doi.org/10.2118/154567-MS.

Moore, T. F., and Slobod, R. L. 1956. “Displacement of Oil by Water-Effect of Wettability, Rate, and Viscosity on Recovery.” Paper presented at the Fall Meeting of the Petroleum Branch of AIME, New Orleans, Louisiana, October 1955. https://dx.doi.org/10.2118/502-G.

Moore, T. F. and Slobod, R. L. 1956. “The Effect of Viscosity and Capillarity on Displacement of Oil by Water.” Producers Monthly 20 (10): 20–30.

Morel, D., Vert, M., Jouenne, S. et al. 2008. “Polymer Injection in Deep Offshore Field: The Dalia Angola Case.” Paper presented at the SPE Annual Technical Conference and Exhibition, Denver, Colorado, USA, September. https://dx.doi.org/10.2118/116672-MS.

Morrow, N. R. 1990. “Wettability and Its Effect on Oil Recovery.” Journal of Petroleum Technology **42** (12): 1476–1484. https://doi.org/10.2118/21621-PA.

Poulsen, A., Shook, G. M., Jackson, A. et al. 2018. “Results of the UK Captain Field Interwell EOR Pilot.” Paper presented at the SPE Improved Oil Recovery Conference, Tulsa, Oklahoma, USA, April. https://dx.doi.org/10.2118/190175-MS.

Qi, P., Ehrenfried, D. H., Koh, H. et al. 2017. “Reduction of Residual Oil Saturation in Sandstone Cores by use of Viscoelastic Polymers.” SPE Journal **22** (02): 447–458. https://doi.org/10.2118/179689-PA.

Sagyndikov, M., Mukhambetov, B., Orynbasar, Y. et al. 2018. “Evaluation of Polymer Flooding Efficiency at Brownfield Development Stage of Giant Kalamkas Oilfield, Western Kazakhstan.” Paper presented at the SPE Annual Caspian Technical Conference and Exhibition, Astana, Kazakhstan, October. https://dx.doi.org/10.2118/192555-MS.

Sagyndikov, M. S., Kushekov, R. M., and Seright, R. S. 2022. “Review of Important Aspects and Performances of Polymer Flooding versus ASP Flooding.” Bulletin of the Karaganda University. “Chemistry” Series 107 (3): 35–55. https://doi.org/10.31489/2022Ch3/3-22-13.

Sandengen, K., Melhuus, K., and Kristoffersen, A. 2017. “Polymer ‘Viscoelastic Effect’; Does It Reduce Residual Oil Saturation.” Journal of Petroleum Science and Engineering **153**: 355–363. https://doi.org/10.1016/j.petrol.2017.03.029.

Seright, R. S., Fan, T., Wavrik, K. et al. 2011. “New Insights into Polymer Rheology in Porous Media.” SPE Journal **16** (01): 35–42. https://doi.org/10.2118/ 129200-PA.

Seright, R. S. 2017. “How Much Polymer Should Be Injected During a Polymer Flood? Review of Previous and Current Practices.” SPE Journal **22** (01): 1–18. https://doi.org/10.2118/179543-PA.

Seright, R. S., Wang, D., Lerner, N. et al. 2018. “Can 25-Cp Polymer Solution Efficiently Displace 1,600-Cp Oil During Polymer Flooding?” SPE Journal **23** (06): 2260–2278. https://doi.org/10.2118/190321-PA.

Seright, R. S., Wavrik, K. E., Zhang, G. et al. 2021. “Stability and Behavior in Carbonate Cores for New Enhanced-Oil-Recovery Polymers at Elevated Temperatures in Hard Saline Brines.” SPE Reservoir Evaluation & Engineering **24** (01): 1–18. https://doi.org/10.2118/200324-PA.

Seright, R. S. and Wang, D. 2023. “Polymer Flooding: Current Status and Future Directions.” Petroleum Science **20** (02): 910–921. https://doi.org/10.1016/j.petsci.2023. 02.002.

Seright, R. S., Azad, M. S., AlAbdullah, M. B. et al. 2023. “Effect of Residual Oil Saturation and Salinity on HPAM Rheology in Porous Media.” Paper presented at the SPE Annual Technical Conference and Exhibition, San Antonio, Texas, USA, 16−18 October. https://doi.org/10.2118/215060-MS.

Seright, R.S., Jouenne, S., and Aften, C. 2025. “Effect of Salinity and Hardness on Hydrolyzed Polyacrylamide Rheology in Sandstone.” SPE Journal **30** (08): 4908-4926. https://doi.org/10.2118/224231-PA.

Shankar, V., Jain, S., Mishra, A. et al. 2018. “Polymer Injection Pilots in Bhagyam Oil Field and Full Field Polymer Development Planning.” Paper presented at the SPE EOR Conference at Oil and Gas West Asia, Muscat, Oman, March. https://doi.org/10.2118/190472-MS.

Shuler, P. J., Kuehne, D. L., Uhl, J. T. et al. 1987. “Improving Polymer Injectivity at West Coyote Field, California.” SPE Reservoir Engineering **2** (03): 271–280. https://doi.org/10.2118/13603-PA.

Sorbie, K. S. 1991. “Polymer-Improved Oil Recovery.” London, UK: Blackie and Son Ltd.

Souayeh, M., Al-Maamari, R. S., Karimi, M. et al. 2021. “Wettability Alteration and Oil Recovery by Surfactant Assisted Low Salinity Water in Carbonate Rock: The Impact of Nonionic/Anionic Surfactants.” Journal of Petroleum Science and Engineering **197**: 108108. https://doi.org/10.1016/j.petrol.2020.108108.

Souayeh, M., Al-Maamari, R. S., Mansour, A. et al. 2022. “Injectivity and Potential Wettability Alteration of Low-Salinity Polymer in Carbonates: Role of Salinity, Polymer Molecular Weight and Concentration, and Mineral Dissolution.” SPE Journal **27** (01): 840–863. https://doi.org/10.2118/208581-PA.

Stegemeier, G. L. 1976. “Mechanisms of Entrapment and Mobilization of Oil in Porous Media.” AICRE Mtng, 81st, Missouri, 55–91.

Taber, J. J. 1969. “Dynamic and Static Forces Required to Remove a Discontinuous Oil Phase from Porous Media Containing Both Oil and Water.” SPE Journal **9** (01): 3–12. https://doi.org/10.2118/2098-PA.

Taber, J. J. 1980. “Research on Enhanced Oil Recovery: Past, Present and Future.” Pure and Applied Chemistry **52** (05): 1323–1347. https://doi.org/10.1351/pac198052051323.

Taber, J. J. 1981. “Research on Enhanced Oil Recovery: Past, Present and Future.” In Surface Phenomena in Enhanced Oil Recovery, edited by D. O. Shah. Boston, Massachusetts, USA: Springer.

Urbissinova, T. S., Trivedi, J. J., and Kuru, E. 2010. “Effect of Elasticity During Viscoelastic Polymer Flooding: A Possible Mechanism of Increasing the Sweep Efficiency.” Journal of Canadian Petroleum Technology **49** (12): 49–56. https://doi.org/10.2118/133471-PA.

Vermolen, E. C., Haasterecht, M. J., Masalmeh, S. K. et al. 2011. “Pushing the Envelope for Polymer Flooding Towards High-Temperature and High-Salinity Reservoirs with Polyacrylamide Based Ter-Polymers.” Paper presented at the SPE Middle East Oil and Gas Show and Conference, Manama, Bahrain, September. https://doi.org/10.2118/141497-MS.

Vermolen, E. C., Haasterecht, M. J., and Masalmeh, S. K. 2014. “A Systematic Study of the Polymer Visco-Elastic Effect on Residual Oil Saturation by Core Flooding.” Paper presented at the SPE EOR Conference at Oil and Gas West Asia, Muscat, Oman, March. https://doi.org/10.2118/169681-MS.

Wang, D., Cheng, J., Yang, Q. et al. 2000. “Viscous-Elastic Polymer Can Increase Microscale Displacement Efficiency in Cores.” Paper presented at the SPE Annual Technical Conference and Exhibition, Dallas, Texas, USA, 1−4 October. https://doi.org/10.2118/63227-MS.

Wang, D., Wang, G., and Xia, H. 2011. “Large Scale High Visco-Elastic Fluid Flooding in the Field Achieves Higher Recoveries.” Paper presented at SPE Enhanced Oil Recovery Conference, Kuala Lampur, Malaysia, 19−21 July. https://doi.org/10.2118/144294-MS.

Zaitoun, A., Makakou, P., Blin, N. et al. 2012. “Shear Stability of EOR Polymers.” SPE Journal **17** (02): 335–339. https://doi.org/10.2118/141113-PA.

Zechner, M., Clemens, T., Suri, A. et al. 2015. "Simulation of Polymer Injection under Fracturing Conditions—an Injectivity Pilot in the Matzen Field, Austria." SPE Reservoir Evaluation & Engineering **18** (02): 236–249. https://doi.org/10.2118/169043-PA.

Zhao, Y., Yin, S., Seright, R. S. et al. 2021. "Enhancing Heavy-Oil-Recovery Efficiency by Combining Low-Salinity-Water and Polymer Flooding." SPE Journal **26** (03): 1535–1551. https://doi.org/10.2118/204220-PA.

## Appendix

| Flood type | Darcy flux rate (ft/day) | Stabilized Pressure gradient (psi/ft) | End Point So | RF/IRF (%) | Nc |
|---|---|---|---|---|---|
| Water Flood (RF 48.66%) | 2 | 4.98 | 0.316 | 47.65% | 1.16E-06 |
| | 4 | 11.34 | 0.316 | 0.00% | 2.63E-06 |
| | 8 | 20.65 | 0.314 | 0.34% | 4.80E-06 |
| | 16 | 35.00 | 0.312 | 0.34% | 8.13E-06 |
| | 32 | 58.79 | 0.312 | 0.00% | 1.37E-05 |
| | 64 | 100.05 | 0.310 | 0.34% | 2.33E-05 |
| Glycerin Flood | 0.05 | 8.55 | 0.310 | 0.00% | 1.17E-06 |
| 2500 ppm AN-125 low salinity polymer solution (IRF 12.55%) | 0.05 | 1.50 | 0.310 | 0.00% | 3.33E-07 |
| | 0.075 | 2.02 | 0.310 | 0.00% | 4.50E-07 |
| | 0.1 | 2.52 | 0.310 | 0.00% | 5.61E-07 |
| | 0.25 | 7.10 | 0.310 | 0.00% | 1.58E-06 |
| | 0.5 | 16.13 | 0.310 | 0.00% | 3.59E-06 |
| | 1 | 32.36 | 0.310 | 0.00% | 7.20E-06 |
| | 5 | 179.89 | 0.304 | 1.01% | 4.00E-05 |
| | 10 | 388.87 | 0.295 | 1.48% | 8.65E-05 |
| | 50 | 1965.02 | 0.263 | 5.37% | 4.37E-04 |
| | 100 | 3358.96 | 0.234 | 4.70% | 7.47E-04 |

Table A-1—Summary of core flooding recovery results from core NIL-06, imposed, measured, and calculated parameters used in CDC generation.

| Flood type | Darcy flux rate (ft/day) | Stabilized Pressure gradient (psi/ft) | End Point So | RF/IRF (%) | Nc |
|---|---|---|---|---|---|
| Water Flood (RF 49.85%) | 2 | 5.35 | 0.281 | 49.23% | 1.18E-06 |
| | 4 | 12.26 | 0.279 | 0.38% | 2.69E-06 |
| | 8 | 23.85 | 0.278 | 0.23% | 5.24E-06 |
| | 16 | 40.82 | 0.278 | 0.00% | 8.97E-06 |
| | 32 | 67.56 | 0.278 | 0.00% | 1.48E-05 |
| | 64 | 113.16 | 0.278 | 0.00% | 2.49E-05 |
| Glycerin Flood | 0.05 | 7.77 | 0.278 | 0.00% | 1.00E-06 |
| 4000 ppm AN-125 high salinity polymer solution (IRF 10.62%) | 0.05 | 0.68 | 0.278 | 0.00% | 1.44E-07 |
| | 0.075 | 1.06 | 0.278 | 0.00% | 2.26E-07 |
| | 0.1 | 1.53 | 0.278 | 0.00% | 3.26E-07 |
| | 0.25 | 5.54 | 0.278 | 0.00% | 1.18E-06 |
| | 0.5 | 12.59 | 0.278 | 0.00% | 2.69E-06 |
| | 1 | 28.35 | 0.278 | 0.00% | 6.05E-06 |
| | 5 | 225.75 | 0.273 | 0.77% | 4.82E-05 |
| | 10 | 522.88 | 0.267 | 1.15% | 1.12E-04 |
| | 50 | 2420.59 | 0.227 | 7.31% | 5.16E-04 |
| | 100 | 4035.29 | 0.219 | 1.38% | 8.61E-04 |

Table A-2—Summary of core flooding recovery results from core NIL-09, imposed, measured, and calculated parameters used in CDC generation.

| Term | Unit conversion factor |
|---|---|
| Core absolute permeability ($k$) | 1 mD ≈ 9.86923E-16 $m^2$ |
| Differential pressure gradient ($\Delta P/L$ ) | 1 psi/ft ≈ 22620.5948 ($N/m^2$)/m |
| IFT ($\sigma$) | 1 mN/m = 0.001 N/m |

Table A-3—Unit conversion factors used in calculating the capillary number